ChemPubSoc Europe

DOI: 10.1002/celc.201700154

CHEMELECTROCHEM Articles

Rational Method for Improving the Performance of Lithium-Sulfur Batteries: Coating the Separator with Lithium Fluoride

Chao Li,[a] Peng Zhang,*[b] Jianhui Dai,[b] Xiu Shen,[a] Yueying Peng,[a] Yiyong Zhang,[a] and Jinbao Zhao*[a, b]

Sulfur, as a cathode material in lithium−sulfur batteries, has a very high theoretical specific capacity of 1675 mAh g^{-1}, but there is still a large challenge, because of polysulfides' (PSs) that cause a severe shuttle effect. To suppress this effect, a simple way of modifying separator by introducing lithium fluoride (LiF) as a coating layer was developed. Owing to the interaction between LiF and dimethoxymethane (DME, an electrolyte solvent), a dense and viscous sol layer was formed that suppresses PSs passing from the cathode to the anode. The presence of this layer was confirmed by using Fourier transform infrared spectroscopy, thermogravimetric/differential thermogravimetric, and scanning electron microscopy. The linear sweep voltammetry test had shown that the LiF-coated separator had a wide electrochemical window above 5 V vs. Li/Li$^+$, and the cell assembled with the LiF-coated separator exhibited an excellent cycling performance with a capacity retention rate of 69.3%. Even without $LiNO_3$ as an electrolyte additive, a high coulombic efficiency of 93% after 200 cycles at 0.2 C was achieved.

1. Introduction

The appearance of rechargeable battery brings lots of convenience for our daily life. For example, a large number of devices become portable such as mobile phones, cardiac pacemakers, cameras and laptops, etc. Furthermore, the power of transportation tools like cars, buses and bicycles are being replaced by electric motor to protect the environment and to be convenient. Also, the booming development of the speed and performance of artificial intelligence demands larger energy, while the convenience of portable devices is pursued. Thus, the batteries with high specific energy are in demand. However, the specific capacity of nowadays commercial cathode materials is far from people's demands.[1]

The lithium-sulfur (Li–S) battery has attracted more and more attention,[2] since the sulfur has a high theoretical specific capacity of 1675 mAh g^{-1} with lithium as anode. The value is nearly ten times more than that of the conventional cathodic materials, such as $LiMnO_2$ and $LiFePO_4$, used in the lithium ion batteries. Nevertheless, there are three main obstructions that Li–S batteries are confronted with. Firstly, the natural insulating property of elemental sulfur urges it to be combined with more conductive carbon material, resulting in decreasing energy density of full cell. Secondly, the bulk expanse of S to Li_2S during the discharging process is so huge that the electrochemical performance suffers from the great change of the electrode architecture. The last but the most serious problem is the dissolution of soluble intermediate, polysulfides (PSs), which not only decreases the utilization rate of the active material, but also can shuttle from cathode to anode, causing low coulombic efficiency and lithium anode corrosion, which is called "shuttle effect".[1b,3] To address the "shuttle effect" of Li–S battery, lots of efforts have been devoted to suppress PSs ions migration to anode area through the separator.

As well known that Li–S battery is composed of the sulfur material as a cathode, the Li foil as an anode and the polyolefin membrane as separator, which all are soaked in a liquid electrolyte, which generally is lithium bis(trifluoromethanesulfonyl)imide (LiTFSI) dissolved in a mixture of dimethoxymethane (DME) and 1,3-dioxolane (DOL) (1:1 by volume). Therefore, present researches are focusing on the following four aspects: the cathode modification, the anode protection, the separator modification and the electrolyte additive. Among them, the cathode modification has attracted the most attention. Various metals, metal oxides metal sulfides and polymer were utilized to mix with elemental sulfur for immobilizing the PSs due to these materials could form strong bonding energy with the PSs ions.[2b,4] Also, the physical absorption has the advantage absorbing PSs. In order to make full use of physical absorption, different carbon materials, such as microporous carbon and hollow porous carbon spheres, were manufactured.[4b,5] The effectivity of the methods through modification of anode material and electrolyte additive was also revealed, among which the electrolyte additive, lithium nitrate ($LiNO_3$), was applied extensively.[6] In addition, the interlayer placed between cathode and separator was also

[a] C. Li, X. Shen, Y. Peng, Y. Zhang, Prof. J. Zhao
State Key Lab of Physical Chemistry of Solid Surfaces
Collaborative Innovation Centre of Chemistry for Energy Materials
State-Province Joint Engineering Laboratory of
Power Source Technology for New Energy Vehicle
College of Chemistry and Chemical Engineering, Xiamen University
Xiamen 361005 (P.R. China)
E-mail: jbzhao@xmu.edu.cn
[b] Dr. P. Zhang, J. Dai, Prof. J. Zhao
College of Energy, Xiamen University
Xiamen 361005 (P.R. China)
E-mail: pengzhang@xmu.edu.cn

Supporting information for this article is available on the WWW under http://dx.doi.org/10.1002/celc.201700154

considered to be important to restrict the shuttling of PSs ions to lithium electrode.[7]

The separator is an indispensable component of lithium battery for separating cathode apart from anode and plays an important role for the safety of battery. Researchers have also found that the separator is effective to block the shuttling of PSs ions.[8] Both Nafion and the boron-based single ion conductive separator have been proved to be effective to improve the cycling performance of Li–S battery.[9] Owing to some negatively charged groups on its surface, the graphite oxide coated separator improved cycling performance obviously.[10] Ketjen black-MnO composite has also been coated on separator gaining an excellent performance for Li–S battery.[11] Additionally, the separators coated by Al_2O_3, V_2O_5, and $Li_{1.5}Al_{0.5}Ge_{1.5}(PO_4)_2$, respectively, have also been reported to be applied in the Li–S batteries.[12] Meantime, The concept of "solvation in salt" has been raised, which make use of viscosity of electrolyte to suppress the PSs ion migration,[13] and the quasi-solid state electrolyte has been made through electro-polymerization method to suppress the PSs ion migrating.[14] Nevertheless, the LiTFSI is expensive, thus too much use of LiTFSI will not be an applicable way.

In lithium ion battery with $LiPF_6$-based electrolyte, the LiF is a main compound of solid electrolyte interphase (SEI), which is essential for the stability of battery and has the voltage decomposition window of 5.91 V *vs* Li/Li^+.[15] LiF has also been proven as an additive to improve the columbic efficiency of batteries with carbonate-based electrolyte by Lynden A. Archer's group.[16] And LiF has been reported to own a low barrier energy for surface diffusion of Li ions over the surface of LiF.[17] However, in the ether-based electrolyte, LiF has a very low solubility.[18] Kim et al and Gao utilized lithium bis (fluoromethanesulfonyl)imide (LiFSI) as the lithium salt instead of LiTFSI to in situ form LiF as a protective coating on cathode.[19] In addition, Manthiram' group used LiF formed by fluorinated ether electrolyte to strengthen the stability of SEI on the anode of Li–S cell, improving the cycling performance.[20]

Although achieved excellent performance of Li–S battery, these methods were complex or high-cost. Previous reports reported that LiF could interact with DME as a Lewis alkali through Lewis acid Li atom to form DME(LiF) cluster,[21] and we found that LiF in DME solution could form a semi-transparent sol, and the compound of LiF and DME had a high viscosity (Figure SI1). In the presence of the interaction between LiF and DME, a physical barrier would be formed, and the mobility of liquid would be decreased, all of which would benefit the blocking of PSs. Meanwhile, because of a low barrier energy for surface diffusion of Li ions over the surface of LiF,[17] the migration of Li ions would not be effected obviously. As a result, it could be concluded that using the LiF coating layer to modify the separator for Li–S battery with DME-based electrolyte could suppress the PSs ions due to the interaction between LiF and DME. Furthermore, this coating layer would protect Li anode when it was placed towards Li anode because of high surface energy of LiF.[19a, 22] In this work, the LiF submicronic particles prepared by ball-milling was coated onto commercial lithium ion battery polyolefin separator with the adhesive. The modified separator performed an excellent characteristic for suppressing "shuttle effect". The method coating LiF submicronic particles onto separator is very simple and low-cost, and it is considered to be a promising method for improving performance of Li–S battery.

2. Results and Discussion

The basic features for the separators such as thermal shrinkage and the contact angle tests results were shown in Figure SI2 and SI3. LiF coated separator showed excellent performances on the basic features.

The micro morphology of routine and milled LiF particles were shown in Figure 1a and 1b. After being milled, LiF particles turned into around 300 nm. The surface scanning electron microscope (SEM) images of the pristine separator, the LiF coated separator and SiO_2 coated separator before cycling were showed in Figure 1c, 1d, and 1e, respectively. The uniform pores in the pristine separator could be seen in the Figure 1c, and the pore size of microspores was about 200 nm, which could maintain ionic pathway and avoid the direct contact between cathode and anode. However, the PSs ions could also transfer through these channels resulting in loss of active material sulfur in Li–S battery. After coated with LiF, the surface of separator was covered with submicronic particles with the size of about 300 nm. And the LiF particles were dispersed meanly on the surface of separator. Meanwhile, the surface became smooth in the main, which could make for inhibition of lithium dendritic crystal. The cross-section SEM image of LiF coated separator could be seen in Figure 1f, and the coating layer thickness was uniform around 7 μm. The smooth surface and uniformity thickness of coating layer were important for protecting Li metal, owing to inducing Li ion meanly transferring.[23] In addition, the interface of coating layer and separator membrane was tight, indicating the strong adhesion between the LiF coating layer and membrane. It should be noted that tortuous tunnels had formed obviously, which could play a role of size exclusion effect. Microspores had been

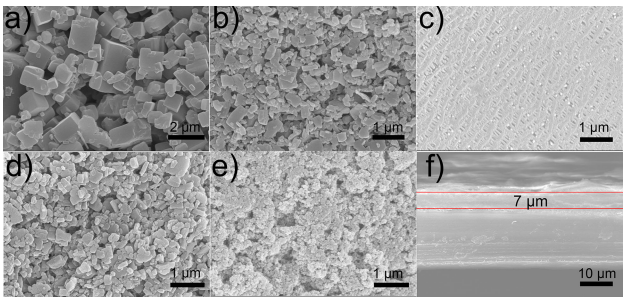

Figure 1. SEM images of a) before being milled LiF particles and b) after being milled LiF particles, as well as the c) pristine separator, d) LiF-coated separator, and e) SiO_2-coated separator before cycling; f) cross-section SEM image of LiF separator before cycling.

proved to be beneficial for suppressing PSs ions by Cui's group.[24]

The Fourier transform infrared spectroscopy (FT-IR) spectra of LiF with DME was measured as shown in the Figure 2. The

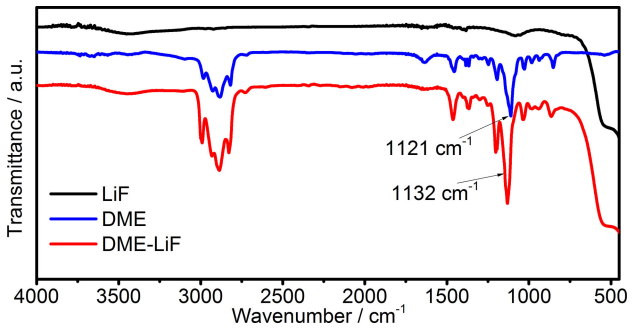

Figure 2. FTIR spectra of LiF, DME, and DME-LiF.

peak at 1121 cm^{-1} was aligned to the vibration of bond C–O–C, and shifted to 1132 cm^{-1} when mixed with LiF obviously. It is because the DME has the high donor number constant of 24[25] as a Lewis alkali, which LiF could interact with through Li atom.[26] The interaction between LiF and DME increased the bond force constant, resulting in the peak shifting. The LiF in DME would become sol-like with a higher viscosity, which would benefit undoubtedly reducing the migration of liquid and suppressing PSs ions.

If a sol layer was formed, saturated vapor pressure of solvent would be decreased, resulting in volatilization slowing down. That would be reflected in the TG and DTG curves. We conducted the measurement of TG testing. In the process, LiF powder by milled method was dried in vacuum oven under 120 °C for 30 h and then mixed with liquid electrolyte. In addition, the mass of LiF powder and liquid electrolyte was as the same as that of pristine separator and liquid electrolyte, so that the condition was kept the same. In Figure 3, the DTG

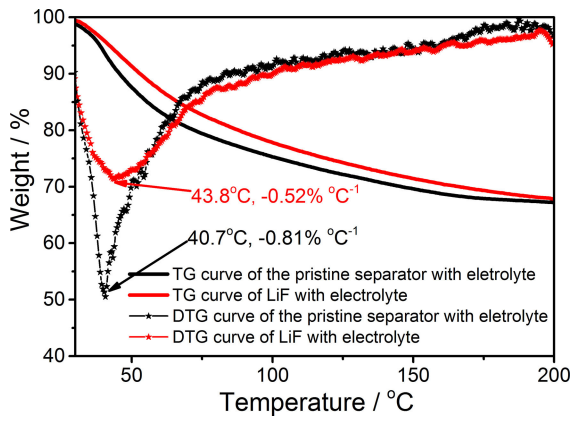

Figure 3. TG and DTG curves of the pristine separator and LiF powder soaked in the same liquid electrolyte.

curve of LiF with liquid electrolyte showed that the maximum evaporation rate and temperature was 0.52% at 43.8 °C, while that of pristine separator soaked in liquid electrolyte was 0.82% at only 40.7 °C. Obviously, the volatilization of LiF soaked liquid electrolyte was slower than that of pristine separator soaked in liquid electrolyte. It was an evidence that the sol layer was formed which could be also seen in Figure SI1.

The lithium ion conductivity of separator soaked in liquid electrolyte reflected migrating rate of lithium ions through the separator which was influenced by pore size and porosity of the separator. The ionic conductivity of LiF coated separator was 5.6×10^{-4} S cm^{-1}, which was a little lower than that of pristine separator of 6.9×10^{-4} S cm^{-1} and SiO_2 coated separator 7.2×10^{-4} S cm^{-1}, That might be attributed to the physical barrier of LiF layer and increased viscosity of electrolyte in the coating layer, which was caused by the interaction between LiF and DME.

The electrochemical window of LiF coated separator, SiO_2 coated separator and pristine separator soaked in liquid electrolyte was investigated via LSV on CHI660E from 1 V to 6 V with the scan rate of 1 mV s^{-1}. As we known, the LiF was stable up to 5.9 V *vs* Li/Li^+. The LSV curves (Figure 4a) of LiF coated separator, SiO_2 coated separator and pristine separator soaked in liquid electrolyte had only one oxidation peak at about 5 V, which was attributed to the decomposition of LiTFSI and solvent. It was noted that the anodic peak for the LiF coated separator soaked in liquid electrolyte shifted to a higher voltage, which should be attributed to the electron affinity of LiF improving the stability of DME. It could also prove the interaction between LiF and DME. Therefore, the LiF coated separator is suitable in the Li–S electrolyte system, whose work voltage window is 1.5 V ~ 3.0 V *vs* Li/Li^+.

Li ion transference number could deliver the feature of separators to hinder anodic ion. The result of Li ion transference number (t_+) of LiF coated separator was shown in figure 4b. Current slowly went down from 0.117 mA to 0.087 mA. The equivalent Randles circuit was used to fit EIS, obtaining that R_0 was 63.8 Ω and R_s 79.2 Ω. So, t_+ was 0.61, which was usually 0.2 ~ 0.4 for the commercial separator.[27] Apparently, the LiF coated separator was efficient for blocking the diffusion of PSs anions.

The electrochemical reversibility of the cells assembled with both LiF coated separator and $LiNO_3$ as electrolyte additive was investigated by the cycle voltammetry (CV) method. Figure 4c showed that the CV curves of cell assembled with LiF coated separator owned two typical cathodic peaks at about 2.3 V and 2.1 V and one anodic peak at about 2.5 V for the Li–S battery system. The cathodic Peak at about 2.3 V was attributed to the reduction from element S to high-ordered polysulfides Li_2S_x ($x \geq 4$), while the peak at about 2.1 V belonged to the transformation from Li_2S_x ($x \geq 4$) to Li_2S_2 and Li_2S.[28] Meantime, the anodic peak at about 2.5 V was attributed to the oxidation of polysulfides to element S or Li_2S_8. From 2th cycle, all of the cathodic and anodic peaks nearly had no shift, suggesting that good reversibility was gained for the cell assembled with LiF coated separator, which indicated that the cell with LiF coated separator had a good reversibility.

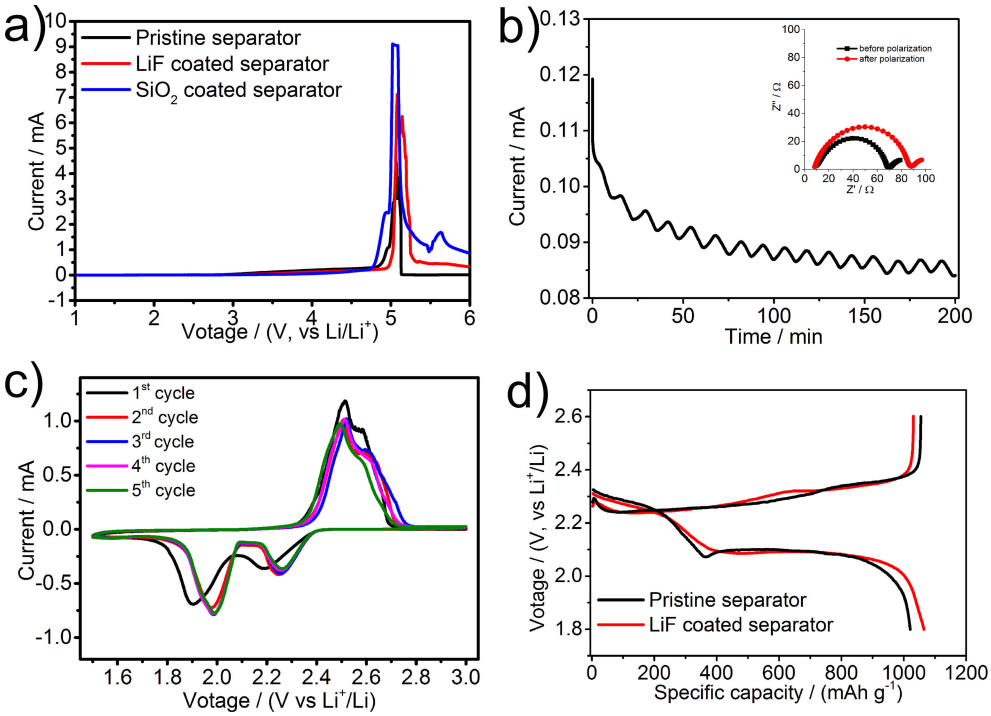

Figure 4. a) LSV curves of the LiF-coated separator, SiO_2-coated separator, and pristine separator soaked with liquid electrolyte at a scan rate of 1 mV s^{-1}. b) Lithium-ion transference number polarization curve of the LiF-coated separator, EIS spectra before and after polarization, and the equivalent Randles circuit. c) CV curves of a Li–S cell with a LiF-coated separator during the first five cycles at a scan rate of 0.1 mV s^{-1}. d) The initial discharge/charge curves of cells assembled with a LiF-coated separator or a pristine separator.

As illustrated in Figure 4d, the initial discharge/charge curves of cells with LiF coated separator and routine separator, respectively, using 1 M LiTFSI in DME/DOL (V:V = 1:1) containing 1 wt% $LiNO_3$ as electrolyte additive at 0.2 C, both owned two typical discharging plateaus of Li–S battery, one about 2.3 V and another about 2.1 V. The discharge/charge plateaus were in corresponding to the peaks in the CV result. The cells with LiF coated separator or pristine separator had the specific discharge capacity of 1064.6 mAh g^{-1} and 1020.6 mAh g^{-1}, respectively. And the charge capacity of cells with LiF coated separator and pristine separator were 1030.5 mAh g^{-1} and 1054.2 mAh g^{-1} respectively. There was no excessive discharge/charge plateau appearing in the curve of the cell assembled with LiF coated separator, compared to that of the cell assembled with pristine separator, indicating the coating of LiF had no any side reaction in the electrochemical reactions corresponding to the LSV measurement for the LiF coated separator. What should be mentioned was that the cell assembled with pristine separator had still an overcharge phenomenon even with $LiNO_3$ as electrolyte additive, but little overcharge phenomenon was found in the cell assembled with LiF coated separator. It could prove the effect of LiF coated separator for suppressing PSs ions.

The cycling performance profiles of cells with the pristine separator and the LiF coated separator were showed in Figure 5a. The cycling performance of the cell with pristine separator was similar to the previous reports.[4c] After three cycles, the specific capacity of cell assembled with LiF coated separator was more stable, compared to the cell with pristine separator which still had a fast decay. After 200 cycles, the discharge capacity of the cell assembled with LiF coated separator was 580.4 mAh g^{-1}, capacity retention rate of 69.3 % based on 3th discharge capacity, but the cell assembled with pristine separator was only 341.4 mAh g^{-1}, capacity retention rate of 37.5 % based on 3th discharge capacity. Cell with LiF coated separator also showed capacity fading. That was because that although LiF coated separator could suppress the PSs shuttling to anode efficiently, PSs could still be dissolved in liquid electrolyte. In the process, PSs could be absorbed in separator and on particles, which could hardly return to the cathode. Therefore, it also made the capacity fade to some extent. It was noted that the discharge capacity of the cell assembled with the SiO_2 coated separator after 200 cycles was only 222.2 mAh g^{-1}, which was due to the coating layer towards Li foil, while SiO_2 could absorb PSs ions which could not be reused, resulting in the bad cycle performance. Accordingly, based on the capacity at 3th cycle, the discharge capacity decay of the cell assembled with pristine separator was 3.03 mAh g^{-1}, while that of the cell assembled with LiF coated separator was only 1.30 mAh g^{-1} per cycle. A better cycling performance was gained obviously. It should be attributed to the blocking effect of LiF coated separator to PSs ions, and the effect stemmed from the sol layer between LiF and DME, not just the microspores formed by LiF particles. And EIS results (Figure SI4) of the cells assemble with pristine separator and LiF coated separator showed using LiF coated separator had nearly no side effect. And the rate performances (Figure 5b) of cells also showed that LiF coating onto separator had no negative impact on rate performance of the cell. In addition, for cell with LiF coated separator gained 752.4 mAh at 0.2 C after 1.6 C cycles and kept an excellent stability.

Meanwhile, the cells with high sulfur loading were also tested (Figure 5c). As same as the cells with low loading sulfur, the cells of high loading sulfur assembled with LiF coated separator showed a more stable performance than that with pristine separator. Meantime, cells assembled with LiF coated

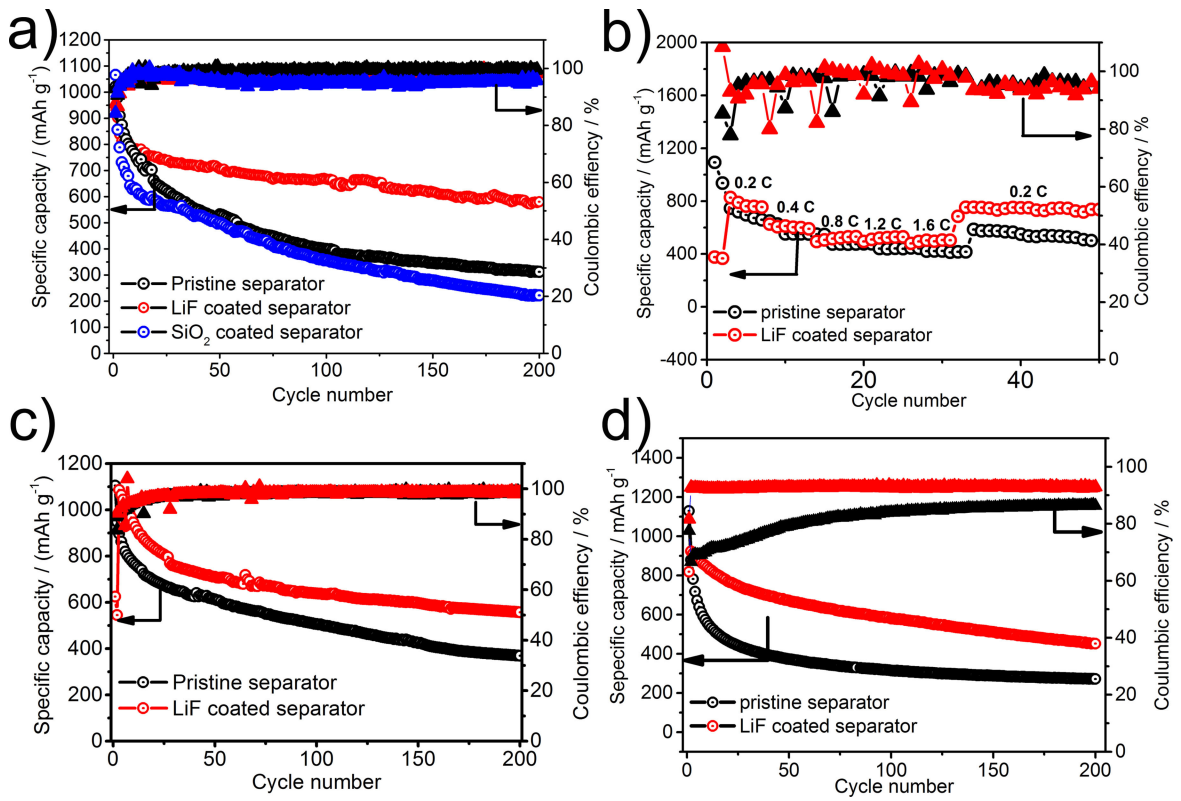

Figure 5. Cycling performance profiles of different cells a) at 0.2 C with $LiNO_3$ as additive, b) at different rates, c) with a high mass load of sulfur of about 3 mg cm^{-1} at 0.04 C, and d) without $LiNO_3$ at 0.2 C.

separator and and pristine separatorwithout $LiNO_3$ as electrolyte additive were also investigated in cycling performance (Figure 5d) respectively,. As a result of PSs ions shuttle effect, the cell assembled with pristine separator had a severe overcharge phenomenon, resulting in a low coulombic efficiency of 79.8% at an average and a quick capacity loss. However, as expected, the cell assembled with LiF coated separator maintained a more stable and higher coulombic efficiency of above 93% without any $LiNO_3$ as electrolyte additive, which was a large improvement in contrast to that of the cell assembled with pristine separator. In order to confirm the capability of LiF coated separator for limiting PSs ions in the cathodic area, visible shuttle effect tests were carried out by the H type glass cell with the separator in its middle, which was easy to replace the LiF coated separator, the SiO_2 coated separator and pristine separator. To guard the coating layer, the front surface was added a layer of pristine separator, meanwhile, two pristine separators were used in the contrasted experiment. 0.1 M Li_2S_6 solution was prepared by mixing Li_2S and pure S at the stoichiometric ratio of 1:5 in DOL and DME (1:1, by volume) under magnetic stirring for 6 h. Both of the left chambers were 0.1 M Li_2S_6 solution, accompanying the right one filled blank electrolyte (DOL and DME, 1:1, by volume). In order to avoid the dissolution of LiF in the large amount of liquid electrolyte, excess LiF powders were put into the solution. Figure 6a, 6b and 6c showed the test results. At the beginning, the color of the right chambers with pristine separator, the SiO_2 coated separator or the LiF coated separator

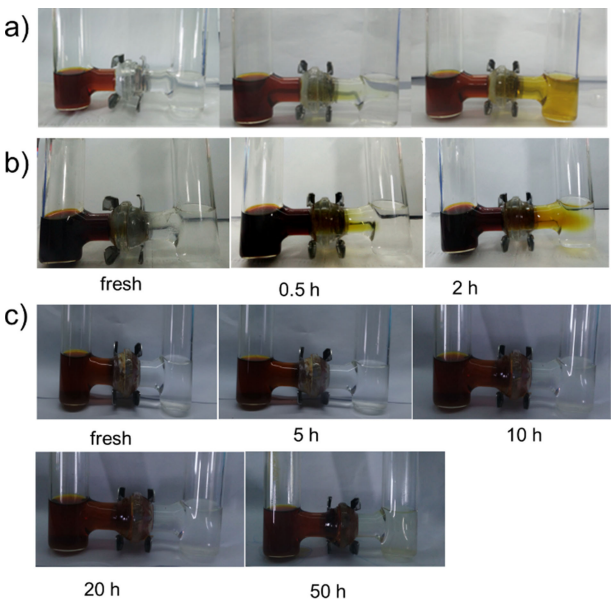

Figure 6. Polysulfide permeation measurements. H-type permeation device with a) the pristine separator, b) the SiO_2-coated separator, and c) the LiF-coated separator.

was the same. However, as expected, after 0.5 h, a color change could be observed in the right one of glass cells with pristine separator and the SiO_2 coated separator, and the color turned darker yellow with the time. Contrastively, nearly no color

change could be seen for the blank cell with LiF coated separator, even after 50 h, little color change could be observed, which could prove that LiF coated separator could suppress PSs ions. Therefore, it could explain the reason why the Li–S cell assembled with LiF coated separator could have a better stability performance and a higher coulombic efficiency.

The shuttle effect of PSs ions would cause corrosion of anode lithium. To detect the effect of LiF coated separator to the anode lithium foil, the lithium foils in cells with LiF coated separator or pristine separator after 150 cycles at full discharged status were taken out after cells were dissembled in Argon-filled glove box. Then, the lithium foils were washed with DME to remove PSs and other substances. After DME on Li foils volatilized fully, the Li foils were transferred quickly into a SEM measurement device. Figure 7a ~ 7d showed the SEM images of

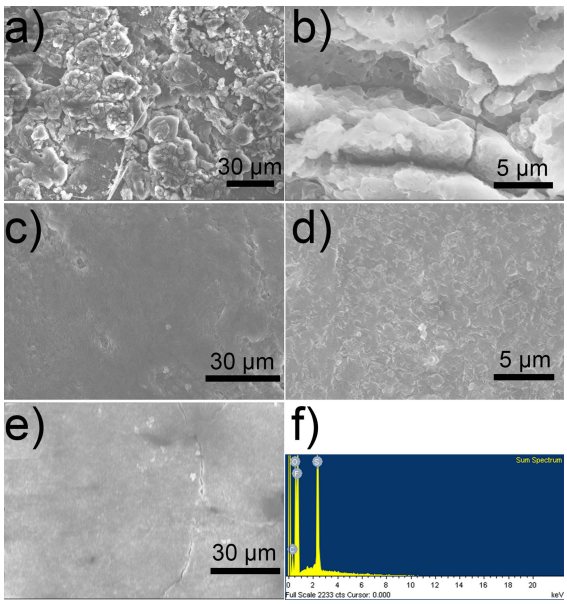

Figure 7. SEM images of Li metal a,b) of cell assembled with the pristine separator and c,d) of cell assembled with the LiF-coated separator, after 150 cycles. e) SEM image and f) energy-dispersive spectroscopy (EDS) of the Li anode after 50 cycles at full discharged status.

lithium foils mentioned above. Severe corrosion could be seen on the surface of lithium foil taken out from the cell assembled with pristine separator (Figure 7a and 7b), which was similar with the previous report,[12a, 29] in which the phenomenon was considered to be caused by the attack from the PSs ions to the lithium metal. In contrast, the surface of lithium foil dissembled from the cell with LiF coated separator (Figure 7c and 7d) maintained a smoother morphology, without lithium hole or dendrite. The absence of lithium hole should be attributed to little PSs ions existing in anode Li foil, and That there was no lithium dendrite should be due to the smooth surface and uniform thickness of coating layer. It could be a powerful proof that the LiF coated separator could suppress the shuttling of PSs and protect anode lithium metal, which could explain that the cell with LiF coated separator gained a more stable cycle performance.

In addition, lithium foil taken out from cell after 50 cycles at discharged status assemble with LiF coated separator whose coating layer was 11 μm was tested, too (Figure 7e, 7f and Table 1). In Figure 7e, thick and dense layer was observed,

Table 1. EDS elemental analysis results.

Element	Weight%	Atomic%
C K	8.73	13.58
O K	12.39	14.47
F K	64.82	63.76
S K	14.06	8.19
Totals	**100.0**	

which might be the interaction between LiF and liquid electrolyte. And EDS results (Table 1) showed that the ratio of S and O element on the surface of the dense layer was nearly in consistent with that in LiTFSI, indicating that little PSs shuttling to the anode. Those indicated that LiF coating on separator could effectively protect lithium.

To further explore the reason why the LiF-coated separator could retard PSs, the SEM images of the pristine separator and the LiF coated separator faced to lithium anode, respectively, was carried out after 50 cycles at full discharged status, which were taken out from the cells disassembled in the argon-filled glove. From Figure 8e and 8f, we could see a compact surface

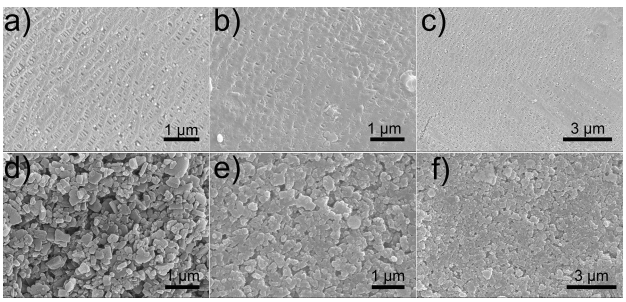

Figure 8. SEM images of a–c) the pristine separator and d–f) the LiF-coated separator taken out of the cells after 50 cycles at discharged status.

of the LiF coated separator, which might be owing to the interaction between LiF and DME. No obvious pores could be observed, that could also explain why the LiF coated separator could suppress shuttling of PSs ions to anode. In contrast, the obvious pores still existed on the surface of the pristine separator taken out from cell dissembled (Figure 8b and 8c). The obvious microspores could be observed compared with the LiF coated separator before cycling (Figure 8a), demonstrating that the dense layer formed in situ because of the interaction between LiF and DME. And the formed dense layer could block the channel for PSs ions. In addition, the lower barrier energy for surface diffusion of lithium ions over the surface of LiF could help the migration of lithium ions. So, the protection for lithium and the suppression for PSs could account for the better cycling performance of cells with the LiF coated separator.

To further prove the suppressing capacity of LiF coated separator to PSs ions, the X-ray photoelectron spectroscopy (XPS) S 2p spectra of the surface of pristine and the LiF coated separators towards anode lithium foil in cells were performed. The fitting criterion was as the previous report[7a,30] and Table SI1 showed comparison between binding energies obtained and that in previous literatures. The value was similar within the allowable range of error, taking the insulating nature of the separators into consideration. Figure 9a and 9b showed the S 2p XPS spectra and fitting results of pristine separator and the LiF coated separator after 10 cycles at fully charged status. The peaks of bridging S and terminal S which were representative of long chained PSs owned a large proportion of the spectra for the pristine separator. It indicated that PSs ions could migrate through pristine separator freely, which could explain the reason of bad cycling performance of the cell assembled with pristine separator. Compared with the pristine separator, little terminal and bridging S could be found for the LiF coated separator, which suggested that little PSs ions shuttled through the LiF coating layer.

3. Conclusions

In summary, the separator coated with LiF had been prepared by simple coating method successfully which had been applied in Li–S battery. The investigation via an electrochemistry window test indicated that the LiF coated separator was suitable in the Li–S battery. The FT-IR, TG and DTG, SEM, SEM-EDS elemental analysis results showed that LiF in DME could form sol, which would be beneficial to the formation of a dense layer to suppress PSs shuttling, through which the lithium ions could migrate freely due to the lower barrier energy for diffusion of lithium ions over the surface of LiF. Using LiF coated separator, the Li–S cell owned an excellent cycling performance with the capacity retention rate of 69.3%. And even without $LiNO_3$ as an electrolyte additive, the high coulombic efficiency of 93% at average after 200 cycles at 0.2 C was gained. The H-type cell test showed that the LiF coated separator could suppress PSs ions obviously. The FTIR and SEM images of separators in cells assembled with pristine and LiF coated separator after cycling demonstrated that the interaction between LiF and DME prompted the formation of a dense layer, which could block PSs ions and allow lithium ions to pass through freely. Therefore, as the Scheme 1 illustrated, there existed PSs passing from cathode to anode in the cell assembled with pristine separator (Scheme 1a), while after coating LiF, with the protection of the coating layer, the PSs ions could not migrate to anode. At the same time, the LiF coating layer could transfer Li ions without influence because of the low barrier energy for diffusion of Li ions over the surface of LiF. The LiF coating layer could play a role that could block the PSs shuttling and allow Li ions to transfer freely. As a simple method to improve the characteristics of Li–S battery, we believe that the LiF coating method will be a promising method in the future.

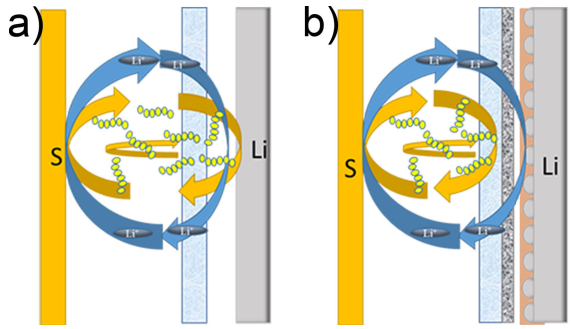

Scheme 1. Schematic configuration of the Li – S cells with a) the pristine separator and b) the LiF-coated separator.

Experimental Section

Material Preparation

The LiF submicronic particles were prepared through ball-milling commercial micro LiF particles 4 g commercial micro LiF powder and a certain amount of acetone were put together to ensure LiF particles all were swelled in acetone, and then was ball-milled to the size of around 300 nm at the speed of 400 rpm for 4 h on the QM-3SP04 planetary ball mill (Nanjing NanDa Instrument Plant), in which the weight of ball (ZrO_2) and LiF particles was 10:1. Then as-prepared LiF particles were mixed with the carboxymethyl cellulose sodium (CMC) and polyvinyl pyrrolidone (PVP) in the water/ethanol (2:1 by weight) solution and the weight ratio of LiF, CMC, PVP was 9:0.5:0.5 and the weight of the three solid was 20%. After that, the mixed solution was continually stirred for 12 h at the ambient

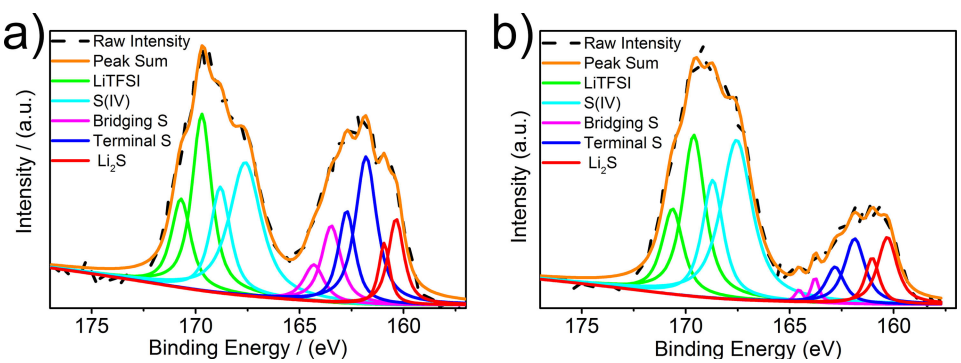

Figure 9. XPS S 2p spectra of a) the pristine separator and b) the LiF-coated separator dissembled from cells.

temperature. The propene polymer (PP) separator (16 μm) (UBE Co., Japan) was selected as the pristine separator, which was coated with the mentioned solution using a doctor blade. Then the separator was dried in the vacuum oven at 50 °C for 24 h. The coating layer was controlled around 7 μm. In order to confirm the effect of LiF coated separator for blocking PSs ions not just stemming from micropores formed between LiF particles, SiO_2 coated separator was performed under the same condition by using 50 nm SiO_2 particles. And for detecting the mechanism, LiF coated separator with 11 μm was also prepared.

Membrane and Material Characterization

The scanning electron microscope (SEM) images and energy dispersive spectrometry (EDS) analysis were performed through HITACHI S-4800 equipment and the cycle voltammetry (CV) spectrum was investigated by CHI660E (Chenhua instrument, Shanghai) with the scan rate of 0.1 mV s^{-1} between 3.0 V and 1.5 V at ambient temperature. The linear sweep voltammetry (LSV) was also using CHI660E with the scan rate of 1 mV s^{-1} from 0 to 6 V *vs* Li/Li^+. X-ray photoelectron spectroscopy (XPS) was measured with the Quantum 2000 (Physical electronics). The photoemission peaks were calibrated using the hydrocarbon contamination peak at 284.8 eV in the C 1 s spectra. Fourier transform infrared spectroscopy (FT-IR) was carried out on ThermoFisher Nicolet iS5, pressing potassium bromide alone or with LiF into sheet, respectively, followed by dropping DME onto the sheet and stewing for 30 min. Then measurement was carried out from 4000 cm^{-1} to 500 cm^{-1}. The thermogravimetric (TG) analysis was achieved on STA 449 F3 Jupiter (Netzsch, Germany) with the heat rate of 2 K min^{-1}.

The lithium ionic conductivity features of pristine separator and LiF coated separator in liquid electrolyte of Li–S cell system were tested by using alternating current (AC) impedance method on Solartron 1286 + 1260 with a frequency ranging from 1 Hz to 100 kHz as the pervious report,[23] using two stainless steel plates to sandwich the soaked separators to form a blocking cell. The lithium ionic conductivity was determined through the following formula:

$$\sigma = L/(S\ R_e) \quad (1)$$

where L is the thickness of the measured separator, R_e is the resistance of the system, and S is the effective area of the electrode.

Estimation of Li^+ transport number ($t_{Li}{}^+$) was conducted through a potentiostatic polarization method on a simulating cell by sandwiching LiF coated separator soaked in liquid electrolyte between two Li foils. Then, ($t_{Li}{}^+$) was calculated using the following equation:

$$t_{Li}^+ = \frac{I_{ss}(\Delta V - I_0 R_0)}{I_0(\Delta V - I_{ss}R_{ss})} \quad (2)$$

where $\triangle V$ is the constant potential of 10 mV, R_0 and R_{ss} are the initial and the final interfacial resistance, I_0 and I_{ss} are the initial and the final current, respectively.

Electrochemical Measurements

The electrochemistry characteristic was investigated by assembling CR2032 type coin cell. The sublimed sulfur with any further processing, the acetylene black and the binder LA132 (Chengdu Indigo Power Sources Co., Ltd Chengdu) were mixed to turn slurry meanly by the mass ratio of 6:3:1, using deionized water as the solvent. Then the slurry was cast onto aluminum foil, followed by drying under vacuum oven under 60 °C for 12 h. Then the cathode sheet was punched into a disc in radius of 6 mm. The sulfur mass loading at unit area of the cathode sheet was controlled at about 0.8 mg and 3.0 mg. The 1 M LiTFSI dissolved in a mixture of dimethoxymethane (DME, Sigma Aldrich, 99.5 %, anhydrous) and 1,3-dioxolane (DOL, Sigma Aldrich, 99.5 %, anhydrous) (1:1 by volume) containing or not containing 1 wt % $LiNO_3$ was as the electrolyte, respectively. The lithium foil was as the anode, and pristine separator, the LiF coated separator and the SiO_2 coated separator were as separator, respectively. The coating layer was placed towards anode lithium. The processes were all operated in Argon-filled glove box (M. Braun Co., Germany). The galvanostatic charge/discharge measurement over the voltage range of 1.8 ~ 2.6 V was initiated on the CT2001 A (Land, Wuhan) battery testing system at ambient temperature. For the cycle performance, the cells were cycled at 0.2 C (1 C = 1675 mA g^{-1}), and the cells with high loading sulfur assembled with LiF coated separator and pristine separator were cycled at the current density of 0.04 C. The specific capacities were calculated based on the active material sulfur.

Acknowledgements

The authors gratefully acknowledge financial support from the National Natural Science Foundation of China (Grant Nos. 21503180, 21273185 and 21321062) and the Fundamental Research Funds for the Central Universities (20720170037). The authors would like to deliver their gratitude to Dr. Daiwei Liao for his valuable suggestions.

Conflict of Interest

The authors declare no conflict of interest.

Keywords: lithium-sulfur batteries · separators · coatings · lithium fluoride · shuttle effects

[1] a) X. Ji, L. F. Nazar, *JMCh* **2010**, *20*, 9821–9826; b) A. Rosenman, E. Markevich, G. Salitra, D. Aurbach, A. Garsuch, F. F. Chesneau, *Adv Energy Mater* **2015**, *5*, 1500212.

[2] a) P. G. Bruce, S. A. Freunberger, L. J. Hardwick, J.-M. Tarascon, *Nat Mater* **2012**, *11*, 19–29; b) X. Tao, J. Wang, C. Liu, H. Wang, H. Yao, G. Zheng, Z. W. Seh, Q. Cai, W. Li, G. Zhou, C. Zu, Y. Cui, *Nat Commun* **2016**, *7*; c) G. Xu, B. Ding, J. Pan, P. Nie, L. Shen, X. Zhang, *Journal of Materials Chemistry A* **2014**, *2*, 12662–12676; d) A. Manthiram, Y. Fu, S. H. Chung, C. Zu, Y. S. Su, *Chem Rev* **2014**, *114*, 11751–11787.

[3] D.-W. Wang, Q. Zeng, G. Zhou, L. Yin, F. Li, H.-M. Cheng, I. R. Gentle, G. Q. M. Lu, *Journal of Materials Chemistry A* **2013**, *1*, 9382–9394.

[4] a) Z. Li, J. Zhang, X. W. Lou, *Angew. Chem. Int. Ed. Engl.* **2015**, *54*, 12886–12890; b) G. Zhou, D.-W. Wang, F. Li, P.-X. Hou, L. Yin, C. Liu, G. Q. Lu, I. R. Gentle, H.-M. Cheng, *ENERG ENVIRON SCI* **2012**, *5*, 8901–8906; c) Y. Peng, B. Li, Y. Wang, X. He, J. Huang, J. Zhao, *ACS Appl Mater Interfaces* **2016**; d) P. Xin, B. Jin, H. Li, X. Lang, C. Yang, W. Gao, Y. Zhu, W. Zhang, S. Dou, Q. Jiang, *ChemElectroChem* **2017**, *4*, 115–121.

[5] a) H.-J. Peng, W.-T. Xu, L. Zhu, D.-W. Wang, J.-Q. Huang, X.-B. Cheng, Z. Yuan, F. Wei, Q. Zhang, *Adv. Funct. Mater.* **2016**, *26*, 6351–6358; b) W. Zhou, C. Wang, Q. Zhang, H. D. Abruña, Y. He, J. Wang, S. X. Mao, X. Xiao, *Adv Energy Mater* **2015**, *5*, 1401752; c) X. Ji, K. T. Lee, L. F. Nazar, *Nat Mater* **2009**, *8*, 500–506; d) N. Jayaprakash, J. Shen, S. S. Moganty, A. Corona, L. A. Archer, *Angew. Chem.* **2011**, *123*, 6026–6030; e) H. Ye, Y.-X. Yin, S. Xin, Y.-G. Guo, *Journal of Materials Chemistry A* **2013**, *1*, 6602–6608; f) W.-C. Du, Y.-X. Yin, X.-X. Zeng, J.-L. Shi, S.-F. Zhang, L.-J. Wan, Y.-G. Guo, *ACS Appl Mater Interfaces* **2016**, *8*, 3584–3590; g) W. Li, Z.

Zhang, W. Kang, Y. Tang, C.-S. Lee, *ChemElectroChem* **2016**, *3*, 999–1005; h) L. Carbone, J. Peng, M. Agostini, M. Gobet, M. Devany, B. Scrosati, S. Greenbaum, J. Hassoun, *ChemElectroChem* **2017**, *4*, 209–215.

[6] a) X. Liang, Z. Wen, Y. Liu, M. Wu, J. Jin, H. Zhang, X. Wu, *J. Power Sources* **2011**, *196*, 9839–9843; b) S. S. Zhang, J. A. Read, *J. Power Sources* **2012**, *200*, 77–82; c) F. Wu, J. T. Lee, N. Nitta, H. Kim, O. Borodin, G. Yushin, *Adv Mater* **2015**, *27*, 101–108.

[7] a) A. Vizintin, M. Lozinšek, R. K. Chellappan, D. Foix, A. Krajnc, G. Mali, G. Drazic, B. Genorio, R. Dedryvère, R. Dominko, *Chem Mater* **2015**; b) A. Wang, G. Xu, B. Ding, Z. Chang, Y. Wang, H. Dou, X. Zhang, *ChemElectroChem* **2016**.

[8] a) Y. Xiang, J. Li, J. Lei, D. Liu, Z. Xie, D. Qu, K. Li, T. Deng, H. Tang, *ChemSusChem* **2016**, 3023–3039; b) N. Deng, W. Kang, Y. Liu, J. Ju, D. Wu, L. Li, B. S. Hassan, B. Cheng, *J. Power Sources* **2016**, *331*, 132–155.

[9] a) Q. Tang, Z. Shan, L. Wang, X. Qin, K. Zhu, J. Tian, X. Liu, *J. Power Sources* **2014**, *246*, 253–259; b) J.-Q. Huang, Q. Zhang, H.-J. Peng, X.-Y. Liu, W.-Z. Qian, F. Wei, *ENERG ENVIRON SCI* **2014**, *7*, 347–353; c) I. Bauer, S. Thieme, J. Brückner, H. Althues, S. Kaskel, *J. Power Sources* **2014**, *251*, 417–422; d) J. Conder, A. Forner-Cuenca, E. M. Gubler, L. Gubler, P. Novak, S. Trabesinger, *ACS Appl Mater Interfaces* **2016**, *8*, 18822–18831.

[10] a) J.-Q. Huang, T.-Z. Zhuang, Q. Zhang, H.-J. Peng, C.-M. Chen, F. Wei, *ACS Nano* **2015**, *9*, 3002–3011; b) M. Shaibani, A. Akbari, P. Sheath, C. D. Easton, P. C. Banerjee, K. Konstas, A. Fakhfouri, M. Barghamadi, M. M. Musameh, A. S. Best, T. Ruther, P. J. Mahon, M. R. Hill, A. F. Hollenkamp, M. Majumder, *ACS Nano* **2016**.

[11] X. Qian, L. Jin, D. Zhao, X. Yang, S. Wang, X. Shen, D. Rao, S. Yao, Y. Zhou, X. Xi, *ELECTROCHIM ACTA* **2016**, *192*, 346–356.

[12] a) Q. Wang, Z. Wen, J. Yang, J. Jin, X. Huang, X. Wu, J. Han, *J. Power Sources* **2016**, *306*, 347–353; b) Z. Zhang, Y. Lai, Z. Zhang, K. Zhang, J. Li, *ELECTROCHIM ACTA* **2014**, *129*, 55–61; c) C. Lin, W. Zhang, L. Wang, Z. Wang, W. Zhao, W. Duan, Z. Zhao, B. Liu, J. Jin, *J. Mater. Chem. A* **2016**, *4*, 5993–5998; d) W. Li, J. Hicks-Garner, J. Wang, J. Liu, A. F. Gross, E. Sherman, J. Graetz, J. J. Vajo, P. Liu, *Chem Mater* **2014**, *26*, 3403–3410.

[13] L. Suo, Y.-S. Hu, H. Li, M. Armand, L. Chen, *Nat Commun* **2013**, *4*, 1481.

[14] H. Zhong, C. Wang, Z. Xu, F. Ding, X. Liu, *Scientific Reports* **2016**, *6*, 25484.

[15] a) H. Yildirim, A. Kinaci, M. K. Y. Chan, J. P. Greeley, *ACS Appl Mater Interfaces* **2015**, *7*, 18985–18996; b) S. Chattopadhyay, A. L. Lipson, H. J. Karmel, J. D. Emery, T. T. Fister, P. A. Fenter, M. C. Hersam, M. J. Bedzyk, *Chem Mater* **2012**, *24*, 3038–3043; c) K. Edström, M. Herstedt, D. P. Abraham, *J. Power Sources* **2006**, *153*, 380–384.

[16] S. Choudhury, L. A. Archer, *Advanced Electronic Materials* **2016**, *2*, 1500246.

[17] Y. Ozhabes, D. Gunceler, T. Arias, *arXiv preprint arXiv:1504.05799* **2015**.

[18] J. McBreen, H. S. Lee, X. Q. Yang, X. Sun, *J. Power Sources* **2000**, *89*, 163–167.

[19] a) H. Kim, F. Wu, J. T. Lee, N. Nitta, H.-T. Lin, M. Oschatz, W. I. Cho, S. Kaskel, O. Borodin, G. Yushin, *Adv Energy Mater* **2015**, *5*, 1401792; b) J. J. Hu, G. K. Long, S. Liu, G. R. Li, X. P. Gao, *Chem Commun* **2014**, *50*, 14647–14650.

[20] C. Zu, N. Azimi, Z. Zhang, A. Manthiram, *J. Mater. Chem. A* **2015**, *3*, 14864–14870.

[21] S. Salai Cheettu Ammal, P. Venuvanalingam, *J. Chem. Soc., Faraday Trans.* **1998**, *94*, 2669–2674.

[22] Y. Zhang, J. Qian, W. Xu, S. M. Russell, X. Chen, E. Nasybulin, P. Bhattacharya, M. H. Engelhard, D. Mei, R. Cao, F. Ding, A. V. Cresce, K. Xu, J.-G. Zhang, *Nano Lett.* **2014**, *14*, 6889–6896.

[23] C. Shi, P. Zhang, L. Chen, P. Yang, J. Zhao, *J. Power Sources* **2014**, *270*, 547–553.

[24] H. Yao, K. Yan, W. Li, G. Zheng, D. Kong, Z. W. Seh, V. K. Narasimhan, Z. Liang, Y. Cui, *Energy Environ. Sci.* **2014**, *7*, 3381–3390.

[25] S.-I. Tobishima, H. Yamamoto, M. Matsuda, *ELECTROCHIM ACTA* **1997**, *42*, 1019–1029.

[26] A. Streitwieser, E. G. Jayasree, F. Hasanayn, S. S. H. Leung, *The Journal of Organic Chemistry* **2008**, *73*, 9426–9434.

[27] a) Z. Jin, K. Xie, X. Hong, *RSC ADV* **2013**, *3*, 8889–8898; b) F. Zeng, Z. Jin, K. Yuan, S. Liu, X. Cheng, A. Wang, W. Wang, Y. Yang, *Journal of Materials Chemistry A* **2016**.

[28] R. Xu, J. Lu, K. Amine, *Adv Energy Mater* **2015**, *5*, 1500408.

[29] J.-S. Kim, D.-J. Yoo, J. Min, R. A. Shakoor, R. Kahraman, J. W. Choi, *ChemNanoMat* **2015**, *1*, 240–245.

[30] a) G. Zhou, Y. Zhao, C. Zu, A. Manthiram, *NANO ENERGY* **2015**, *12*, 240–249; b) N. Moreno, Á. Caballero, J. Morales, E. Rodríguez-Castellón, *J. Power Sources* **2016**, *313*, 21–29.

Manuscript received: February 10, 2017
Final Article published: April 12, 2017